Boosting Predictive Accuracy of Single Particle Models for Lithium-Ion Batteries Using Machine Learning

Emmanuel Olugbade[1] and Jonghyun Park[1,2*]
Missouri University of Science and Technology

[1]Department of Mechanical and Aerospace Engineering, Missouri University of Science and Technology, Rolla, Missouri 65401, United States
[2]Department of Electrical and Computer Engineering, Missouri University of Science and Technology, Rolla, Missouri 65401, United States

Abstract:

The accuracy of single particle (SP) models for lithium-ion batteries (LIBs) at high C-rates is constrained by lithium concentration gradients in the electrolyte, which affect ionic conductivity, overpotential, and reaction rates. This study addresses these limitations using extreme gradient boosting (XGBoost) machine learning (ML). By training our ML model with data from a comprehensive electrochemical (P2D) model and performing sensitivity analysis on key battery parameters, we enhance predictive accuracy. Compared to conventional SP and P2D models under constant current loading, our ML-based SP model achieves similar predictive accuracy to P2D, with significant improvements in computational efficiency. Additionally, the ML-based SP model demonstrates improved predictive accuracy under dynamic loading conditions, providing a practical framework for improving battery management and safety.

* Corresponding author

E-mail address: parkjonghy@mst.edu

Lithium-Ion Batteries (LIBs) have revolutionized energy storage technologies, particularly in the realm of electric vehicles (EVs) and hybrid electric vehicles (HEVs). Their unparalleled energy and power density render them indispensable for meeting the ever-growing demands of these transportation sectors[1-2]. However, this widespread adoption has been accompanied by escalating concerns regarding battery safety, thereby underscoring the urgent need for robust battery management system (BMS)[3-4]. Traditional monitoring techniques, relying predominantly on voltage, current, and temperature measurements, have proven insufficient in accurately predicting critical battery parameters such as state of charge (SOC) and state of health (SOH). This inadequacy not only jeopardizes battery performance but also poses significant safety risks. As such, there arises a pressing demand for advanced sensing and monitoring technologies capable of accurately tracking the intricate physical parameters of lithium-ion batteries[5-6]. While high-fidelity electrochemical models such as proposed by Doyle et al.[7] and their several improved versions offer unparalleled insights into battery behavior, their computational complexity presents formidable challenges for real-time BMS implementation[8]. Simplified models like the equivalent circuit model (ECM) have been widely adopted due to their computational efficiency. However, the ECM's limited predictive capabilities, stemming from its oversimplified representation of battery dynamics, necessitate alternative approaches[9]. The single particle (SP) model, derived from comprehensive electrochemical models, strikes a balance between electrochemical and equivalent circuit models for physical modeling of battery and computational efficiency. It employs a small set of ordinary differential equations to explicitly maintain key battery characteristics. Assuming uniform spherical particles and uniform current distribution in both electrodes, the SP model simplifies each electrode to a single particle. While it effectively describes general charge-discharge behavior, it lacks the ability to capture battery dynamics at high C-rates due to the absence of electrolyte physics[10-12]. Different strategies have been proposed to incorporate the SP model with the electrolyte contribution, employing polynomial equations of varying orders[13-16]. Generally, the polynomial order determines the accuracy of the approximation. Higher-order polynomials are expected to provide greater accuracy, although they entail increased computational complexity for coefficient identification. Thus, while higher-order polynomials offer enhanced precision, they also incur greater numerical costs in terms of coefficient determination. Recent advances in battery modeling have leveraged machine learning techniques to significantly improve performance prediction, useful life estimation[17-18], state of charge (SOC) and state of health (SOH) estimation, thereby enhancing predictive accuracy. However, much of the existing research primarily targets performance prediction and computational efficiency within established models, without fundamentally addressing the core design limitations of these models. For instance, Tran *et al*.[19] compare four multivariate multioutput regression ML methods for predicting battery voltage and temperature, evaluating their feasibility and performance. While such studies enhance predictive accuracy, they often do not tackle the underlying architectural constraints of traditional models. In contrast, this manuscript addresses these limitations by focusing on enhancing the SP model architecture for lithium-ion batteries. Specifically, our work aims to overcome the key limitation of inadequate electrolyte dynamics in traditional SP model, offering a more robust and accurate representation of battery behavior.

In this study, we introduce a method to improve the accuracy and efficiency of conventional SP models in predicting electrolyte overpotential and dynamics across various current rates. Our

approach involves integrating the extreme gradient boosting (XGBoost) machine learning (ML) technique into the SP model framework, aimed at enhancing its predictive capabilities. To validate our method, we compared the results obtained from the proposed model with those from a full-order electrochemical model and a conventional SP model. Additionally, we conducted galvanostatic constant discharge tests and dynamic stress tests (DSTs) to demonstrate the accuracy of our enhanced SP model under different operational scenarios. These validation tests confirm the reliability and effectiveness of our proposed approach in improving the predictive capabilities of SP models for lithium-ion batteries.

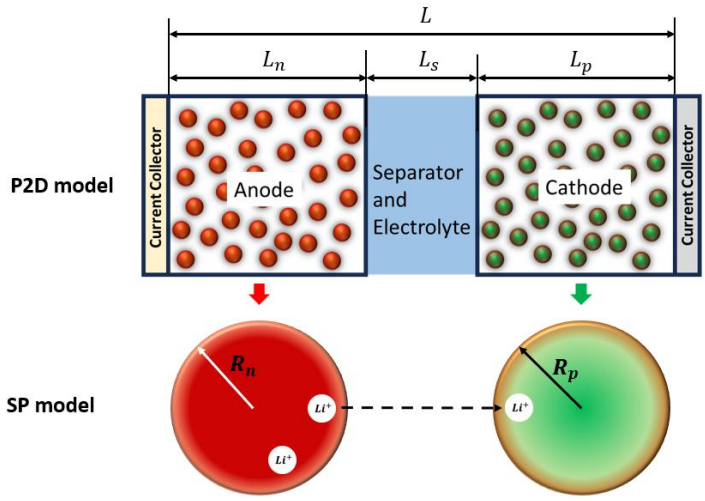

FIG. 1 Schematic of single particle model for Li-ion battery

The conventional SP model relies on two primary assumptions: first, that all particles within an electrode exhibit similar behavior, allowing the entire electrode to be represented by a single spherical particle, as depicted in Fig. 1. Second, it assumes a uniform distribution of current across the electrode particles[11, 20]. Ionic diffusion of Li ion in each particle is governed by Fick's second law:

$$\frac{\partial c_{s,j}(r,t)}{\partial t} = \frac{D_{s,j}}{r^2}\frac{\partial}{\partial r}\left(r^2\frac{\partial c_{s,j}(r,t)}{\partial r}\right) \quad \text{Eq. (1)}$$

The expression describes the solid-phase Li-ion concentration, denoted as $c_{s,j}$, with respect to time (t), radial coordinate (r), and the solid-phase diffusion coefficient ($D_{s,j}$). The subscript $j = p/n$ distinguishes between the positive and negative electrodes. The boundary conditions for the diffusion problem are:

$$D_{s,j}\frac{\partial c_{sj}}{\partial r} = 0 : (r = 0)$$

$$D_{s,j}\frac{\partial c_{sj}}{\partial r} = -J^{Li} : (r = R_j) \quad \text{Eq. (2)}$$

where R_j is the electrode particle radius.

The rate of electrochemical reaction governing the intercalation and deintercalation of lithium ions at the interface between the solid electrode and the electrolyte solution can be characterized using Butler-Volmer kinetics[20].

$$J^{Li} = k_j c_{s,j,max} c_e^{0.5} \left[1 - \frac{c_{s,j,surf}(t)}{c_{s,j,max}}\right]^{0.5} \left(\frac{c_{s,j,surf}(t)}{c_{s,j,max}}\right)^{0.5} \times \left\{exp\left(\frac{0.5F}{RT}\eta_j(t)\right) - exp\left(\frac{-0.5F}{RT}\eta_j(t)\right)\right\} \quad \text{Eq. (3)}$$

The parameter k_j denotes the reaction rate constant, c_e represents the electrolyte concentration, R stands for the universal gas constant, T signifies the temperature, and F is Faraday's constant. The function $c_{s,j,surf}(t)$ is expressed as a function of the particle's surface concentration $c_{s,j,surf}(t) = c_{s,j}(R_j, t)$.

The surface overpotential, η_j is expressed as $\eta_j = \Phi_{1,j} - \Phi_{2,j} - U_j$, where $\Phi_{1,j}$ is the solid-phase potential, $\Phi_{2,j}$ is solution-phase potential, and U_j is the Open Circuit Potential (OCP). The OCP, in general, is a function of the SOC and temperature. The SOC is expressed as the normalized surface concentration, $\frac{c_{s,j,surf}(t)}{c_{j,max}}$. Using reverse hyperbolic function[20], the potential difference is obtained from the reaction rate expression, J^{Li} as

$$\eta_j(t) = \frac{2RT}{F} In\left(m_j(t) + \sqrt{m_j(t) + m_j^2(t) + 1}\right) \quad \text{Eq. (4)}$$

where $m_j(t) = \frac{J^{Li}}{2k_j c_{j,max} c_e^{0.5}\left[1 - \frac{c_{s,j,surf}(t)}{c_{j,max}}\right]^{0.5}\left(\frac{c_{s,j,surf}(t)}{c_{j,max}}\right)^{0.5}}$.

The overall battery terminal voltage is then obtained from the solid-phase potential difference between both ends of the cell[20].

$$V_{cell} = \Phi_{1,p}(t)|_{x=L} - \Phi_{1,n}(t)|_{x=0} \quad \text{Eq. (5)}$$

$$= \left(\eta_p + \Phi_{2,p}(t)|_{x=L} + U_p\right) - \left(\eta_n + \Phi_{2,n}(t)|_{x=0} + U_n\right)$$

$$= U_p\left(\frac{c_{s,p,surf}(t)}{c_{p,max}}\right) - U_n\left(\frac{c_{s,n,surf}(t)}{c_{n,max}}\right) + \frac{2RT}{F}\left(In\left(m_p(t) + \sqrt{m_p^2(t) + 1}\right) - In\left(m_n(t) + \sqrt{m_n^2(t) + 1}\right)\right) + \Phi_{2,p}(t)|_{x=L} - \Phi_{2,n}(t)|_{x=0}$$

The last term in the voltage expression above ($\Phi_{2,p}(t)|_{x=L} - \Phi_{2,n}(t)|_{x=0}$) represents the electrolyte potential difference. In the conventional SP models, the neglect of potential gradients within the electrolyte is a common simplification. In these models, the addition of a resistance term to Butler-Volmer kinetics serves the purpose of modeling interface resistance exclusively, without consideration for potential distribution within the electrolyte. The internal resistance is typically approximated as an ohmic voltage drop, $i_{app}R_{cell}$, where i_{app} denotes the applied current

density. The value of resistance, R_{cell}, is influenced by various intricate mass and charge transfer phenomena. The R_{cell} value is subject to various intricate mass and charge transfer phenomena. Guo et al.[20] proposed an estimation of this resistance based on empirical considerations tied to both the ambient temperature and the current at the battery terminals. In a separate study[21], R_{cell} was posited to be dependent upon electrode ionic conductivities and electrode thicknesses. This assumption underscores a significant limitation of the traditional SP model, as it hinders the ability of model to accurately depict battery dynamics, particularly under high C-rate conditions.

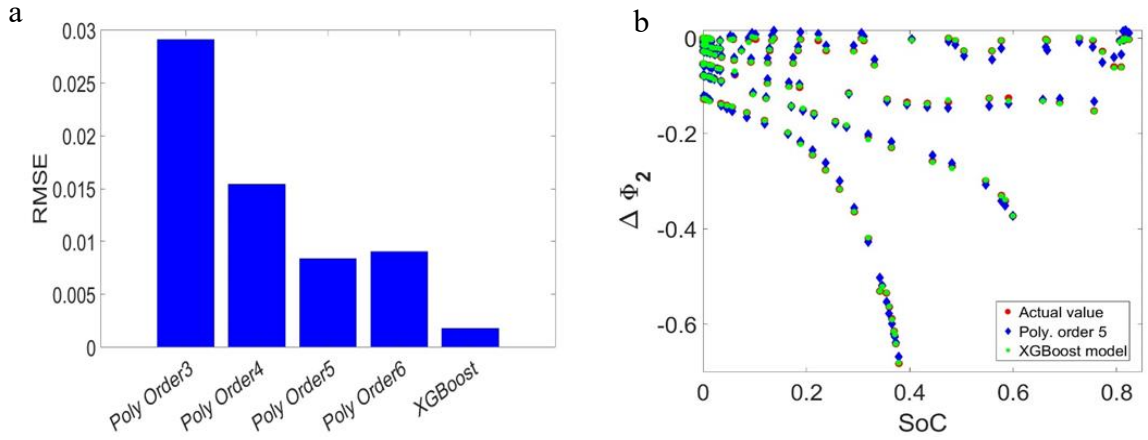

FIG. 2 (a) Root Mean Square Error (RMSE) of polynomial regression models (orders 3 to 6) and XGBoost model. The XGBoost model exhibits the lowest RMSE, indicating improved predictive performance. (b) Predicted $\Delta\Phi_2$ values by the XGBoost model and the 5th order polynomial regression model compared to actual values, showing close alignment with the XGBoost model providing the most accurate predictions.

The main objective of a data-driven methodology is to provide real-time estimations of electrolyte potential within LIBs. Utilizing XGBoost, a ML technique leveraging gradient boosted decision trees, aims to accelerate training procedures, and improve predictive accuracy. The decision to integrate XGBoost into the SP model for electrolyte potential prediction is motivated by its distinct advantages, notably its swift training capabilities and improved accuracy as documented in previous studies[22-23]. Nevertheless, polynomial regression model and XGBoost regression model were compared in terms of predictive accuracy. Polynomial regression was tested with orders 3 to 6, showing decreasing RMSE from 0.0291 for order 3 to 0.00836 for order 5, but a slight increase to 0.00902 for order 6, indicating overfitting at higher orders. The XGBoost model, with a maximum depth of 5 and a learning rate of 0.7, achieved an RMSE of 0.00176, outperforming the best polynomial model (Fig. 2a). Hyperparameter tuning through grid search and 5-fold cross-validation, along with early stopping, validated the XGBoost model's effectiveness. This model was selected for further analysis in this study. The training of the ML model is carried out using dataset obtained from a parametric study based on a comprehensive electrochemical P2D model[7, 24]. Prior to the parametric study, a sensitivity analysis study was conducted to identify key battery parameters influencing electrolyte dynamics, revealing electrolyte conductivity (k), SOC, and C-Rate as pivotal for ML model training. The subsequent parametric investigation involved a diversity of current rates (C-Rate) values: 0.05C, 0.1C, 0.5, 1C, 2C and 5C and adjusting electrolyte conductivity at 80%, 100%, and 120% of its nominal value, with electrolyte potential difference ($\Delta\Phi_2$) designated as the dependent variable. Several discharge cycles were run to obtain

the dataset. Machine learning training utilized 80% of the dataset, with the remaining 20% reserved as a test set. Figure 2 presents a comparison between electrolyte potential predictions generated by the trained machine learning model and those from the P2D model, demonstrating a negligible RMSE of 0.00176. This underscores the exceptional predictive performance of the XGBoost model.

Table I. Comparison of computational times for P2D, SP, and proposed models at 1C Discharge Rate.

Models	Computation time (s)
P2D	43.0
SP	2.0
Proposed model	2.0

Table II. Values of parameters used in the simulations.

Parameter	Value	Description
L_n	100E-6	Thickness of the negative electrode (m) [7]
L_s	52E-6	Thickness of the separator (m) [7]
L_p	183E-6	Thickness of the positive electrode (m) [7]
D_e	7.5E10-11	Diffusion coefficient in electrolyte (m^2/s) [7]
F	96487	Faraday's constant (C/mol) [7]
i_{app}	17.5 ×C-rate	C-rate times 1 C discharge current density (A m−2) [7]
D_n	3.9E-14	Solid-phase Li diffusivity, negative electrode (m^2/s) [7]
D_p	1.0E-13	Solid-phase Li diffusivity, positive electrode (m^2/s) [7]
T	298.15	Ambient temperature (K)
$C_{max,pos}$	22860	Positive maximum concentration (mol/m^3) [7]
$C_{max,neg}$	26390	Negative maximum concentration (mol/m^3) [7]
r_p	8.0E-6	Particle radius, positive electrode (m) [7]
r_n	12.5E-6	Particle radius, negative electrode (m) [7]
k_j	2.0E-6	Reaction rate constant ($m^{2.5}mol^{-0.5}s^{-1}$)[7]

To assess the efficacy of the proposed model, we adopted the LiMn2O4-LiC6 battery chemistry utilized by Doyle et al.[7] Using COMSOL Multiphysics version 6.1, we simulated three models: the P2D model referred to as 'P2D', a conventional SP model referred to as 'SPM', and our proposed machine learning enhanced SP model, referred to as 'XGBoost model'. Each model employed a consistent sampling period of 1 second and a discharge cycle with a stopping condition set at 2.8V to facilitate comparison of computational efficiency. Battery modeling parameters are listed in table II. Table I presents the execution times recorded for each model in the COMSOL program. Notably, the computational times for the SP model (2.0 s) and the proposed model (2.0 s) were identical, contrasting with the P2D model's computational time (43.0 seconds). To assess the model's performance under dynamic loading conditions, simulation of the Dynamic Stress Test (DST) was conducted. This test, designed by the United States Advanced Battery Consortium for evaluating EV and HEV batteries,[25-26] features current profiles with high C-Rate values reaching

up to 6C. Our model was trained up to 5C, necessitating extrapolation for higher C-Rate values. Figure 3 shows the voltage profiles for DST loading, comparing the results with those obtained from conventional SP and P2D models. Notably, our model demonstrates a notably accurate prediction even at extrapolated current values, outperforming the SP model. This accuracy demonstrates that our model generalizes effectively beyond its training data, delivering reliable predictions even at higher current rates. At 6C, the conventional SP model encounters difficulties due to its inability to accurately capture steep gradients in electrolyte potential, increased ionic resistance, and localized potential drops within the electrodes. These limitations lead to reduced accuracy at high C-rates. In contrast, our model, which is trained to handle conditions up to nearly 6C, addresses these challenges. By incorporating considerations for electrolyte potential variations and ionic resistance, our model provides improved generalization and prediction accuracy under high current rates.

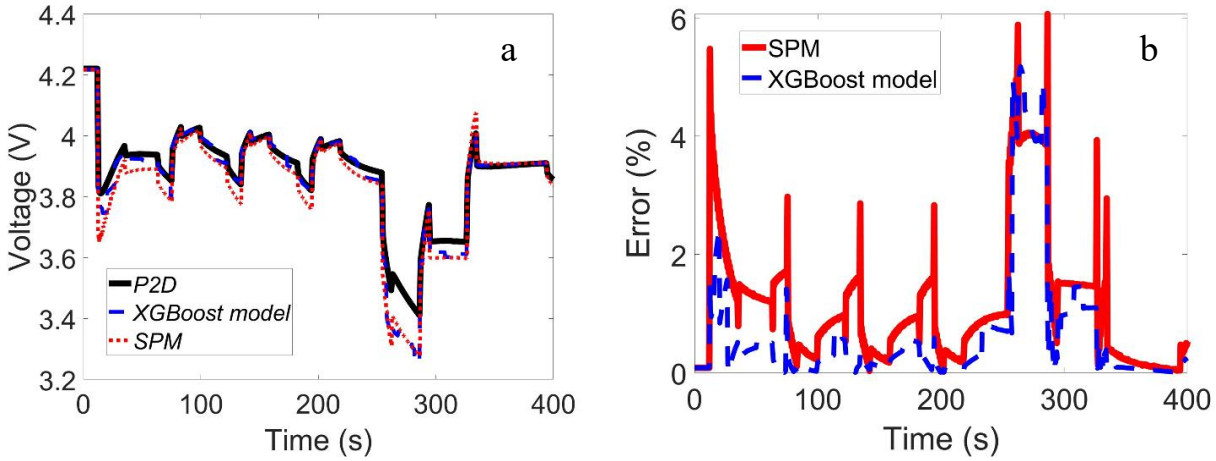

FIG. 3 Evaluation of voltage profiles (3a) and percentage errors (3b) for the SP model and the proposed XGBoost model, compared to the P2D model under dynamic stress test (DST) loading. The P2D model is shown in black, the SP model in red, and the proposed XGBoost model in green. Error plots are colored red for the SP model and blue for the XGBoost model.

In this section, we conducted simulations across three models, spanning cell voltage from 4.2 to 2.8 V for 0.2C, 1C, and 5C C-Rate values. We then compared outcomes from both conventional and proposed SP models with those from the P2D model as illustrated in Fig. 4. Notably, Figures 4a and 4b exhibited good agreement between the conventional and proposed SP models and P2D model results, with a percentage error below 0.3%. However, at higher C-rates, the proposed SP model results (RMSE of 0.00178 for 1C and 0.0122 for 5C) closely aligned with the P2D model compared to the conventional SP model results (RMSE of 0.00239 for 1C and 0.0175 for 5C), as shown in Figs. 4c to 4f. This discrepancy at higher C-rates is attributed to the increasing error in the electrolyte potential difference with rising C-rates, as discussed previously. During the DST, modern batteries, particularly for HEVs, may operate at current loads up to and exceeding 5C. The 5C rate case (Figs. 4e and 4f) demonstrated a significant increase in error rate for the conventional SP model compared to the proposed SP model. In summary, results from the proposed SP model aligned well with those from the P2D model.

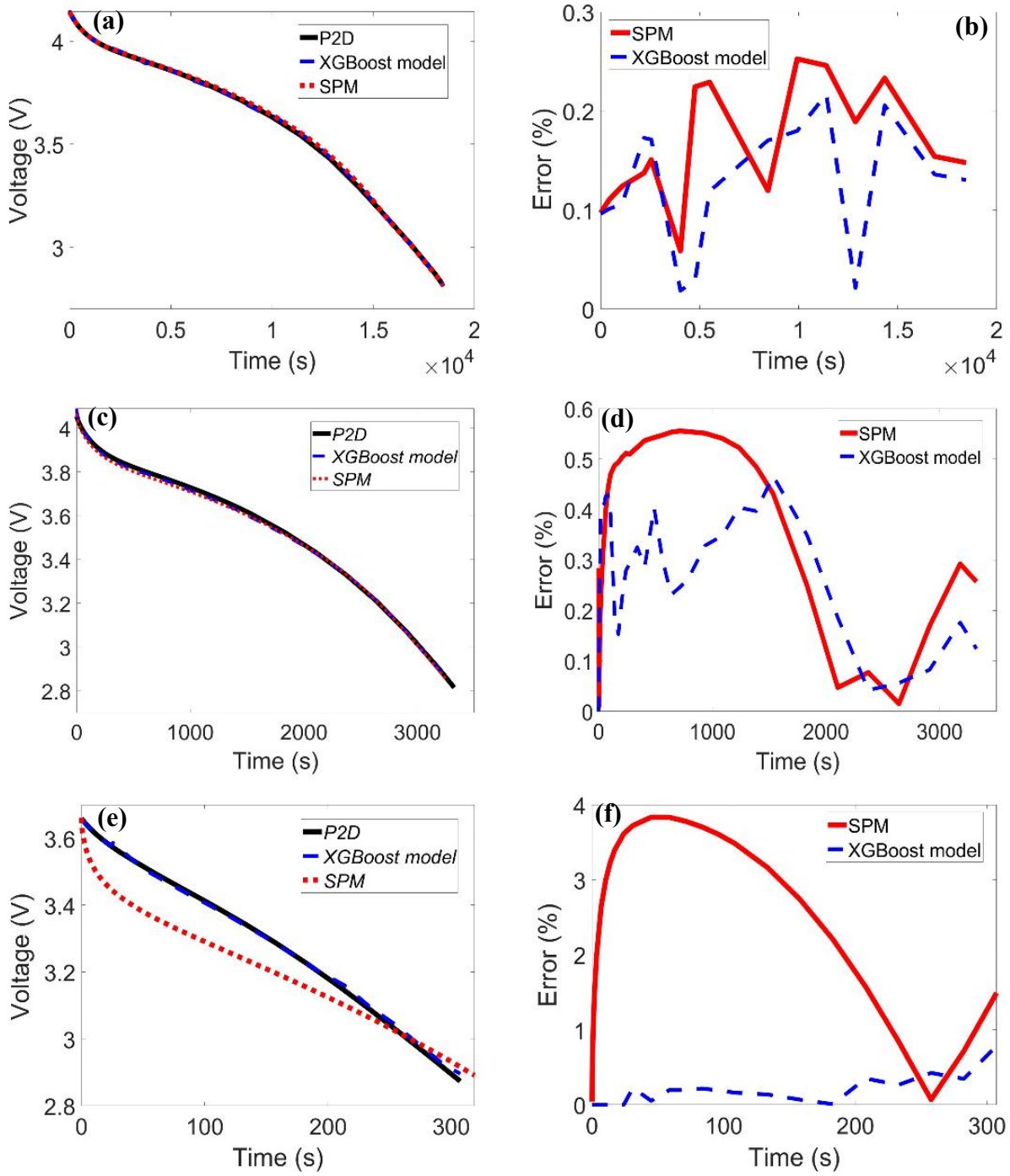

FIG. 4 Comparison of voltage responses and percentage errors for the P2D, SP, and proposed XGBoost models during discharge cycles at 0.2C (a and b), 1C (c and d), and 5C (e and f). The percentage error is consistently higher for the SP model compared to the proposed XGBoost model, indicating greater accuracy of the XGBoost model across all current rates.

Analysis of the electrolyte potential difference in the cell was conducted and plotted in Fig. 5(a,b). The conventional SPM model exhibited a static electrolyte potential indicated by a horizontal line in the plot, highlighting the absence of electrolyte dynamics in the model. In contrast, the proposed model demonstrated changing electrolyte potential values around those obtained from the higher-order P2D model, indicating improved fidelity to real-world conditions. The error plot further revealed an initial percentage error in the SPM model exceeding 80%, underscoring the enhancements introduced by the proposed model. At the onset of discharging, an initial drop in electrolyte potential occurs due to the ohmic drop, which is a result of the increased demand for ions to migrate from the anode to the cathode. This ohmic drop arises from the internal resistance within the battery. Following this initial decrease, the potential typically stabilizes as the battery continues to deliver current to the load. The SP model does not capture this ohmic drop and the associated dynamic response, whereas the proposed model effectively addresses these factors.

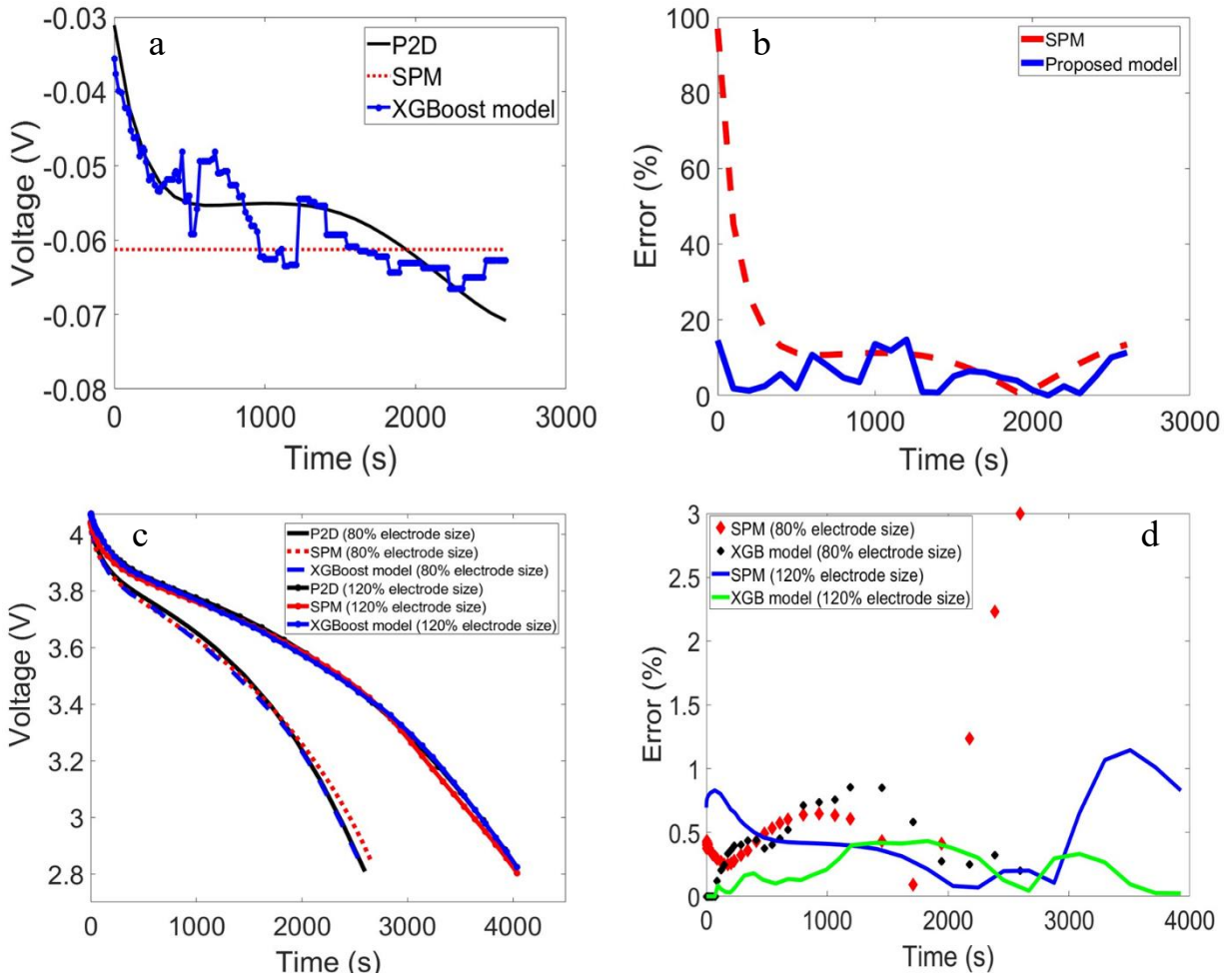

FIG. 5 Analysis of electrolyte potential and voltage profiles. (a) Comparison of electrolyte potential in the P2D model (black curve), the proposed model, and the SP model (horizontal line). (b) Error analysis for the SP model and proposed model, with larger errors observed in the SP model. (c) Discharge voltage profiles for electrode thicknesses of 80% and 120% of nominal value over time. (d) Percentage error for

the SP model and proposed model relative to the P2D model, showing divergence of the SP model towards the end of discharge for both electrode thicknesses.

Electrode thickness variations were implemented to assess the sensitivity of the developed model. Both anode and cathode thicknesses were adjusted to 80% and 120% of nominal values during discharge at a 1C current load. Reducing electrode thickness correspondingly decreased cell capacity, accelerating voltage discharge due to reduced active material volume. Conversely, increasing electrode thickness extended voltage discharge times across all models, including the developed machine learning-enhanced model (Fig. 5(c,d)). Figure 5(c) depicts the voltage discharge profiles under varied electrode thicknesses. Despite these variations, the developed model maintained predictive accuracy comparable to the P2D model. The error plot (Fig. 5(d)) indicates that deviations from the P2D model were minimized in the developed model. However, the largest discrepancies were observed with thinner electrodes. This trend can be attributed to the reduced volume of active material in thinner electrodes, which accelerates charge depletion and amplifies the effects of modeling assumptions, such as the lumped ohmic drop term in the SP model. Generally, the SP model shows a higher percentage error toward the end of the discharge profile. This discrepancy arises from the pronounced electrolyte potential gradient that develops as the concentration gradient increases. As the battery discharges, ions are consumed in electrochemical reactions, which decreases the ion concentration near the electrode surfaces. This reduction creates a larger concentration difference between the depleted regions and the bulk electrolyte, resulting in a steeper electrolyte potential gradient towards the end of the discharge cycle. The SP model does not capture this behavior, whereas the proposed model effectively accounts for it.

In conclusion, this study introduces a data-driven approach using XGBoost to estimate electrolyte potential in LIBs through the single particle (SP) model. Integrating XGBoost improves both predictive accuracy and computational efficiency compared to traditional Physics-based P2D models. Training on a dataset derived from a comprehensive parametric study based on the P2D model achieved a minimal RMSE of 0.00176 for estimating electrolyte potential dynamics. This demonstrates the model's performance across discharge rates up to 5C and varying electrolyte conductivities. Simulation results using COMSOL Multiphysics confirm the effectiveness of the XGBoost-enhanced SP model under different discharge rates and dynamic loading conditions, including the DST. Compared to the conventional SP model, the XGBoost-enhanced approach consistently shows improved performance with lower errors, particularly at high C-rates. Analysis of electrolyte potential dynamics reveals clear improvements with the XGBoost-enhanced SP model, capturing similar to those observed in higher-fidelity P2D models. This advancement signifies closer alignment with real-world electrolyte behaviors. In summary, integrating XGBoost into the SP model framework represents a significant step forward in battery modeling. This approach not only enhances predictive capabilities but also offers insights critical for optimizing LIB design and performance in applications such as electric vehicles and grid-scale energy storage systems.

ACKNOWLEDGEMENTS

The authors gratefully acknowledge the financial support of the National Science Foundation (Grant Numbers: 2230770 and 2028992)

REFERENCES

1. Nykvist, B.; Nilsson, M., Rapidly falling costs of battery packs for electric vehicles. *Nature climate change* **2015,** *5* (4), 329-332.
2. Armand, M.; Tarascon, J.-M., Building better batteries. *nature* **2008,** *451* (7179), 652-657.
3. Srinivasan, R.; Demirev, P. A.; Carkhuff, B. G.; Santhanagopalan, S.; Jeevarajan, J. A.; Barrera, T. P., Thermal safety management in Li-ion batteries: Current issues and perspectives. *Journal of The Electrochemical Society* **2020,** *167* (14), 140516.
4. See, K.; Wang, G.; Zhang, Y.; Wang, Y.; Meng, L.; Gu, X.; Zhang, N.; Lim, K.; Zhao, L.; Xie, B., Critical review and functional safety of a battery management system for large-scale lithium-ion battery pack technologies. *International Journal of Coal Science & Technology* **2022,** *9* (1), 36.
5. Verbrugge, M. W.; Koch, B. J., Electrochemical analysis of lithiated graphite anodes. *Journal of The Electrochemical Society* **2003,** *150* (3), A374.
6. Smith, K.; Wang, C.-Y., Solid-state diffusion limitations on pulse operation of a lithium ion cell for hybrid electric vehicles. *Journal of power sources* **2006,** *161* (1), 628-639.
7. Doyle, M.; Fuller, T. F.; Newman, J., Modeling of galvanostatic charge and discharge of the lithium/polymer/insertion cell. *Journal of the Electrochemical society* **1993,** *140* (6), 1526.
8. Andrea, D., *Battery management systems for large lithium-ion battery packs*. Artech house: 2010.
9. Dees, D.; Gunen, E.; Abraham, D.; Jansen, A.; Prakash, J., Electrochemical modeling of lithium-ion positive electrodes during hybrid pulse power characterization tests. *Journal of the Electrochemical Society* **2008,** *155* (8), A603.
10. Ning, G.; Popov, B. N., Cycle life modeling of lithium-ion batteries. *Journal of The Electrochemical Society* **2004,** *151* (10), A1584.
11. Santhanagopalan, S.; Guo, Q.; Ramadass, P.; White, R. E., Review of models for predicting the cycling performance of lithium ion batteries. *Journal of power sources* **2006,** *156* (2), 620-628.
12. Subramanian, V. R.; Diwakar, V. D.; Tapriyal, D., Efficient macro-micro scale coupled modeling of batteries. *Journal of The Electrochemical Society* **2005,** *152* (10), A2002.
13. Guduru, A.; Northrop, P. W.; Jain, S.; Crothers, A. C.; Marchant, T. R.; Subramanian, V. R., Analytical solution for electrolyte concentration distribution in lithium-ion batteries. *Journal of Applied Electrochemistry* **2012,** *42*, 189-199.
14. Luo, W.; Lyu, C.; Wang, L.; Zhang, L., An approximate solution for electrolyte concentration distribution in physics-based lithium-ion cell models. *Microelectronics Reliability* **2013,** *53* (6), 797-804.
15. Rahimian, S. K.; Rayman, S.; White, R. E., Extension of physics-based single particle model for higher charge–discharge rates. *Journal of Power Sources* **2013,** *224*, 180-194.
16. Baba, N.; Yoshida, H.; Nagaoka, M.; Okuda, C.; Kawauchi, S., Numerical simulation of thermal behavior of lithium-ion secondary batteries using the enhanced single particle model. *Journal of Power Sources* **2014,** *252*, 214-228.
17. Sun, H.; Jiang, H.; Gu, Z.; Li, H.; Wang, T.; Rao, W.; Wang, Y.; Pei, L.; Yuan, C.; Chen, L., A novel multiple kernel extreme learning machine model for remaining useful life prediction of lithium-ion batteries. *Journal of Power Sources* **2024,** *613*, 234912.
18. Li, X.; Yu, D.; Byg, V. S.; Ioan, S. D., The development of machine learning-based remaining useful life prediction for lithium-ion batteries. *Journal of Energy Chemistry* **2023,** *82*, 103-121.
19. Tran, M. K.; Panchal, S.; Chauhan, V.; Brahmbhatt, N.; Mevawalla, A.; Fraser, R.; Fowler, M., Python-based scikit-learn machine learning models for thermal and electrical performance prediction of high-capacity lithium-ion battery. *International Journal of Energy Research* **2022,** *46* (2), 786-794.
20. Guo, M.; Sikha, G.; White, R. E., Single-particle model for a lithium-ion cell: Thermal behavior. *Journal of The Electrochemical Society* **2010,** *158* (2), A122.

21. Di Domenico, D.; Stefanopoulou, A.; Fiengo, G., Lithium-ion battery state of charge and critical surface charge estimation using an electrochemical model-based extended Kalman filter. **2010**.
22. Dineva, A.; Csomós, B.; Sz, S. K.; Vajda, I., Investigation of the performance of direct forecasting strategy using machine learning in State-of-Charge prediction of Li-ion batteries exposed to dynamic loads. *Journal of Energy Storage* **2021,** *36*, 102351.
23. Song, S.; Zhang, X.; Gao, D.; Jiang, F.; Wu, Y.; Huang, J.; Gong, Y.; Liu, B.; Huang, Z. In *A hierarchical state of charge estimation method for lithium-ion batteries via xgboost and kalman filter*, 2020 IEEE International Conference on Systems, Man, and Cybernetics (SMC), IEEE: 2020; pp 2317-2322.
24. Subramanian, V. R.; Boovaragavan, V.; Ramadesigan, V.; Arabandi, M., Mathematical model reformulation for lithium-ion battery simulations: Galvanostatic boundary conditions. *Journal of The Electrochemical Society* **2009,** *156* (4), A260.
25. Silva, C.; Ross, M.; Farias, T., Evaluation of energy consumption, emissions and cost of plug-in hybrid vehicles. *Energy Conversion and Management* **2009,** *50* (7), 1635-1643.
26. He, H.; Xiong, R.; Fan, J., Evaluation of lithium-ion battery equivalent circuit models for state of charge estimation by an experimental approach. *energies* **2011,** *4* (4), 582-598.